WATER RESOURCES RESEARCH, VOL. 33, NO. 12, PAGES 2951–2965, DECEMBER 1997

Linearity of basin response as a function of scale in a semiarid watershed

David C. Goodrich, Leonard J. Lane, Rose M. Shillito, and Scott N. Miller
Southwest Watershed Research Center, USDA–Agricultural Research Service, Tucson, Arizona

Kamran H. Syed
Department of Hydrology and Water Resources, University of Arizona, Tucson

David A. Woolhiser
Ft. Collins, Colorado

Abstract. Linearity of basin runoff and peak response as a function of watershed scale was examined for a set of 29 nested semiarid watersheds within the U.S. Department of Agriculture–Agricultural Research Service Walnut Gulch Experimental Watershed, located in southeastern Arizona. Watershed drainage areas range from 1.83×10^3 to 1.48×10^8 m^2 (0.183–14800 ha), and all stream channels are ephemeral. Observations of mean annual runoff, database-derived 2- and 100-year peak runoff rates, ephemeral channel area, and areal rainfall characteristics derived from 304 events were examined to assess the nature of runoff response behavior over this range of watershed scales. Two types of distributed rainfall-runoff models of differing complexity were applied to a subset of the watersheds to further investigate the scale-dependent nature of the collected data. Contrary to the conclusions of numerous studies in more humid regions, it was found that watershed runoff response becomes more nonlinear with increasing watershed scale, with a critical transition threshold area occurring roughly around the range of 3.7×10^5 to 6.0×10^5 m^2 (37–60 ha). The primary causes of increasingly nonlinear response are the increasing importance of ephemeral channel losses and partial storm area coverage. The modeling results indicate that significant error will result in model estimates of peak runoff rates when rainfall inputs from depth area-frequency relationships are applied beyond the area of typical storm coverage. For runoff modeling in Walnut Gulch and similar semiarid environments, explicit treatment of channel routing and transmission losses from channel infiltration will be required for watersheds larger than the critical drainage area.

1. Introduction

Two primary types of linearity in basin response will be discussed. They are the classical definition from systems theory of proportionality and the definition from *Huang and Willgoose* [1993], which defines linearity of runoff response as a function of drainage basin scale through interpretation of the following equations:

$$V = aA^b \tag{1}$$

$$\mathrm{Qp} = cA^d \tag{2}$$

where V is the mean annual runoff volume, Qp is the basin peak discharge associated with a specified return period, A is the drainage basin area (basin-scale parameter), a and c are regression coefficients, and b and d are exponents. *Huang and Willgoose* [1993] offer a physical interpretation for exponents b and d as measures of the degree to which a basin retards, filters, or diminishes the transformation from rainfall into runoff. Larger exponents imply a lesser degree of basin influence or retardation. When b or $d = 1.0$ the watershed response is linear, implying that the runoff volume and peak flow from a watershed is simply the sum of the volumes or peak flows from smaller subwatersheds forming the overall watershed. *Leopold et al.* [1964] report that in natural basins, values of d range from 0.65 to 1.0. *Benson*'s [1962] results indicated that $d = 0.85$ for 164 watersheds (~2.5–26,000 km^2) in the humid New England region and later that [*Benson*, 1964] $d = 0.59$ for 219 watershed (~2.5–91,000 km^2) in the largely semiarid regions of Texas and New Mexico for a return period of 50 years. Benson noted that d tends to (1) decrease with increasing watershed area and aridity, (2) decrease for increasing return period, and (3) increase with the number of watershed and climatic variables employed in a multivariate regression on peak runoff rate. *Alexander* [1972] suggested an average value for $d = 0.7$ but also noted that estimates of the exponent depend on the range of A as well as the return period and climate of the regions. Using runoff and peak flow per unit area, *Murphey et al.* [1977] found values of $b = -0.20$ and $d = -0.38$ using data from 11 watersheds on Walnut Gulch for the average runoff volume and mean peak discharge during the period of record, respectively. In the context of using runoff volumes or peak rate in $[V^3/T]$ (not per unit area) as (1) and (2) are stated above, their results suggest $b = 0.80$ and $d = 0.62$. *Gupta and Waymire* [1989] offer the physical interpretation of the

Paper number 97WR01422.
0043-1397/97/97WR-01422$09.00

exponent d as the fraction of area of a basin contributing to peak discharge.

Huang and Willgoose [1993] applied a grid-based hydrologic model to a synthetic basin with synthetic spatially uniform rainfall varying from 2 to 220 mm/hr for a fixed duration of 1.5 hours to investigate the dependence of watershed response on basin scale (drainage area). They found that basin scale plays a significant role in runoff response and that the commonly observed power law functions relating peak rate to drainage area (equation (2)) and time to peak to drainage area are applicable. They argue that the regression coefficients and exponents are independent of watershed area and that the value of the exponents are strongly influenced by watershed retardation and diffusive effects as well as by the watershed geomorphology. For a given rainfall intensity, *Huang and Willgoose* [1993] also conclude that the exponents for the peak rate and time to peak versus area power law relations depend on rainfall intensity, with watershed response becoming more linear with increasing intensity.

The second form of linearity is the classical definition from systems theory of proportionality and superposition, where an increase in input (rainfall) results in a proportional increase in output (runoff), and the outputs from different inputs can be superimposed [*Maidment*, 1992; *Dooge*, 1959; *U.S. Department of Agriculture–Agricultural Research Service* (*USDA-ARS*), 1973]. In this context the nonlinear nature of watershed excess runoff response for a given watershed area has been recognized for some time [*Minshall*, 1960; *Chow*, 1964]. *Minshall* [1960] analyzed rainfall-runoff observations from several small experimental watersheds (10.9–117 ha) in Illinois and noted the high degree of nonlinearity and time variance in runoff response. The degree of nonlinearity is further compounded if the relationship between total rainfall and observed runoff is examined as the threshold nonlinearities associated with infiltration, interception, and depression storage come into play. *Chow* [1964], in an overview of several studies which evaluated watersheds ranging in size from 130 to 368,000 ha, concluded that for a given basin, nonlinearity of runoff response exists with respect to storm and seasonal variations. However, a number of studies have concluded that runoff response becomes more linear with increasing basin scale [*Anderson et al.*, 1981; *Dooge*, 1982; *Beven et al.*, 1988; *Wang et al.*, 1981; *Gupta et al.*, 1986]. This trend was also alluded to by *Minshall* [1960], who noted a more linear degree of runoff response for a larger (117 ha) watershed as compared to his initial analysis on a 10.9-ha watershed. *Wang et al.* [1981, p. 545] noted that "linear rainfall-runoff transformations have been observed to provide satisfactory predictions of the direct surface runoff from 'large' basins." The still-common practice of utilizing unit hydrograph methods for consulting and design purposes attests to this observation [*Maidment*, 1992].

Wang et al. [1981] developed a quasi-linear representation of basin outflow using an instantaneous response function (IRF) that is a generalization of the geomorphic instantaneous unit hydrograph (GIUH) [*Rodriguez-Iturbe and Valdes*, 1979]. In this procedure, rainfall intensity dependence of GIUH parameters, which results in nonlinear behavior in the rainfall-runoff transformation, is introduced. Using this approach, the mean holding time of a basin may be estimated as a function of rainfall intensity. *Wang et al.*'s [1981] analysis of data from four basins ranging in scale from 0.104 to 2670 km^2 indicated increasing linearity in basin runoff response with increasing basin scale.

Robinson et al. [1995] also utilized the IRF approach in a largely theoretical study of the scale effects on watershed response. In their study the IRF approach was extended by combining a physically based hillslope response model (hillslope IRF) with a geomorphologically based network response model (network IRF). The combined model was then applied to three nested New Zealand watersheds to investigate the transition from hillslope to network-dominated runoff response. Spatially uniform but variable intensity rainfall inputs and steady state watershed response were used with the combined IRF models to examine the relative effects of basin scale on advection (via the wave celerity) and dispersion (hillslope, geomorphic, and hydrodynamic). They found that the majority of the nonlinearity in watershed runoff response was concentrated in the dependence of the wave celerity on the effective rainfall intensity. In contrast to studies indicating an increase in linearity of basin response with increasing area, *Robinson et al.* [1995] conclude that the nonlinearity in watershed response was equally great in small or large watersheds.

With the exception of one basin in a semiarid region of central Venezuela, all the basins studied by *Robinson et al.* [1995], *Wang et al.* [1981], and *Minshall* [1960] were in humid regions. The primary objective of this study was to test the hypothesis of increasing linearity in basin runoff and peak flow response with increasing basin scale in a well-instrumented semiarid watershed with ephemeral stream channels. Three sets of analyses were carried out to address this objective. In section 2 analyses of observed hydrologic data and basin characteristic data from a series of 29 nested watersheds are presented. Two distributed hydrologic models with different levels of complexity are then utilized as interpretive tools to acquire further insight into the nature of the observations presented in section 2. In section 3 the quasi-distributed hydrologic model developed by *Lane* [1982, 1983] is applied with design storm inputs across a range of scales within the nested watershed network. Estimated peak flows are compared to database-derived peak flow estimates at two different return periods. In section 4 analyses are presented using the more complex KINEROS [*Woolhiser et al.*, 1990; *Smith et al.*, 1995] distributed hydrologic model on a subset of four watersheds. The principal of proportionality is investigated over a range of watershed scales to obtain further insight into the possible role of several hydrologic processes in determining the observations of section 2.

2. Analysis of Hydrologic Observations

The Study Area

Observations were obtained from the 149-km^2 USDA-ARS Walnut Gulch Experimental Watershed, located in southeastern Arizona (31°43′N, 110°00′W) (Figure 1). The watershed is representative of approximately 60 million ha of brush- and grass-covered rangeland found throughout the semiarid southwest and is in a transition zone between the Chihuahuan and Sonoran Deserts. Elevation of the watershed ranges from 1250 to 1585 m above mean sea level (MSL), with the lower two-thirds of the watershed dominated by desert shrub steppe species which transition into desert grasslands on the upper portion of the watershed. Soils are generally well-drained, calcareous, gravelly loams with large percentages of rock and gravel at the soil surface. Cattle grazing is the primary land use, along with mining, limited urbanization, and recreation. Mean annual temperature at Tombstone, located within the watershed, is 17.6°C, and mean annual precipitation is 324 mm, with

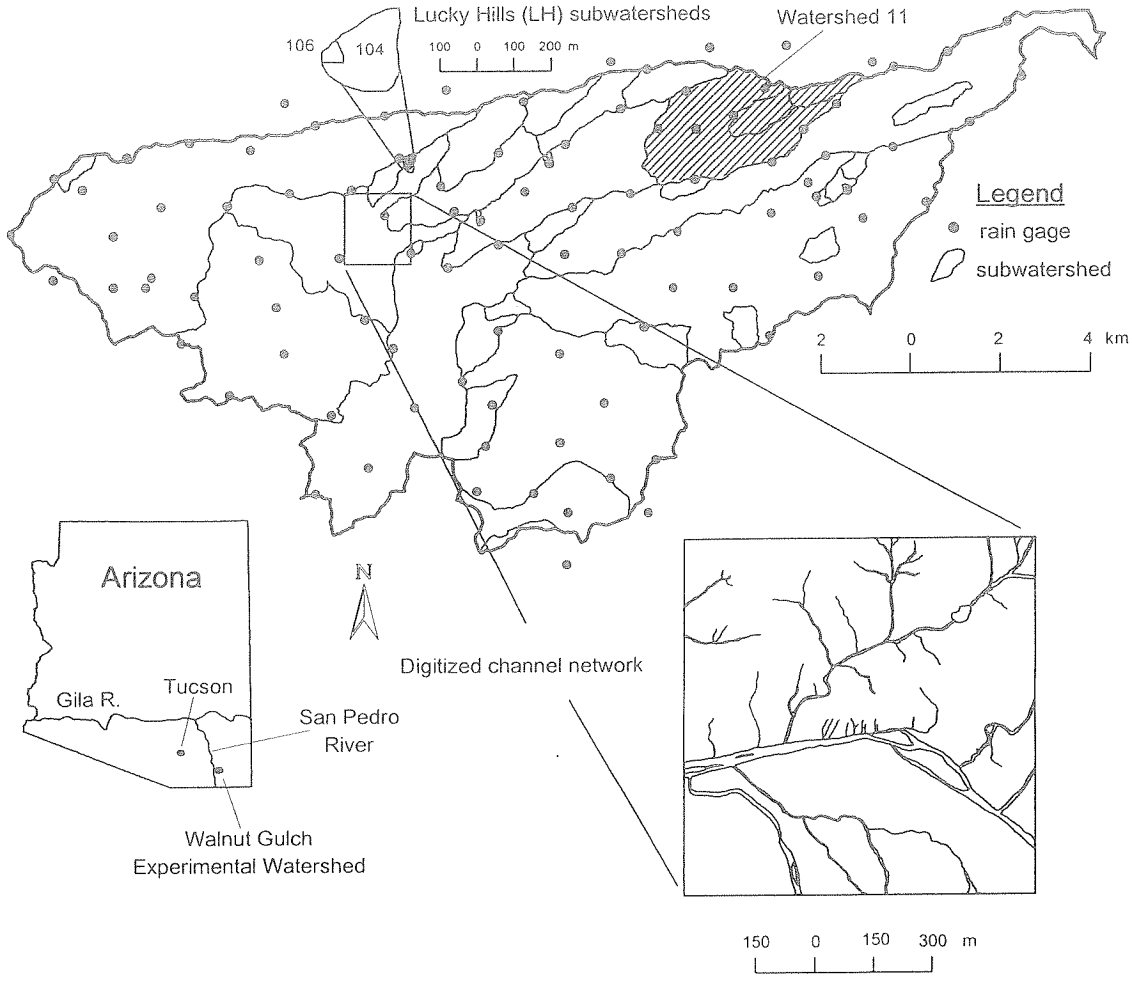

Figure 1. USDA-ARS Walnut Gulch Experimental Watershed: location map, rain gauge and watershed locations, and example of digitized channel polygons.

considerable seasonal and annual variation in precipitation. Approximately two thirds of the annual precipitation on the Walnut Gulch Watershed occurs as high-intensity, convective thunderstorms of limited areal extent. Winter rains (and occasional snow) are generally low-intensity events associated with slow-moving cold fronts and are typically of greater areal extent than summer rains. Runoff is generated almost exclusively from convective storms during the summer monsoon season via infiltration excess. Channel transmission losses play a critical role in Walnut Gulch runoff generation processes [*Lane*, 1985; *Boughton and Stone*, 1985; *Renard et al.*, 1993]. Figure 2 illustrates a typical rainfall event and the substantial decreases in both runoff volume and peak flow rate resulting from ephemeral channel losses as the flood hydrograph progresses downstream from flume 6 to flume 2 to the outlet of the watershed, at flume 1. Depth to groundwater ranges from 50 m at the lower end to 145 m in the central portions of the watershed. For a more detailed description of the watershed see *Renard et al.* [1993].

Instrumentation

Rainfall is currently recorded on a continuous basis at 85 (down from a historic high of 91) locations using recording weighing rain gauges. Runoff from small (<40 ha) watersheds is measured using various gauging structures. These structures include broad-crested V notch weirs, H flumes, and supercritical flow flumes. Data from eight of these watersheds are included in this study. At intermediate scales (roughly 40–300 ha) runoff is measured at stock pond impoundments with stage recorders, surveyed stage-volume relationships, and sharp-crested weirs to gauge pond overflow. Data from 10 watersheds draining into stock ponds is included in the present study. Because stock ponds typically do not spill runoff water during storm, their drainage area was excluded from larger watersheds in which they were nested. At larger scales (roughly 300–14,800 ha at the watershed outlet) runoff is measured with specially developed flumes using a design known as the Walnut Gulch supercritical flume [*Gwinn*, 1970; *Smith et al.*, 1982]. Runoff data from 11 such flumes is included herein. In total, these stations provide runoff from 29 nested watersheds whose drainage area ranges in scale from 0.2 to 13,100 ha (pond impoundment areas removed).

Runoff, Channel Area, Storm Coverage, and Peak Flow Observations

Mean annual runoff volumes were computed for a common 11-year period (1969–1979) of record for the 29 watersheds (Table 1). These data were plotted as solid squares as a function of contributing watershed area (top portion of Figure 3). Generally, the relationship follows a power law in the form of

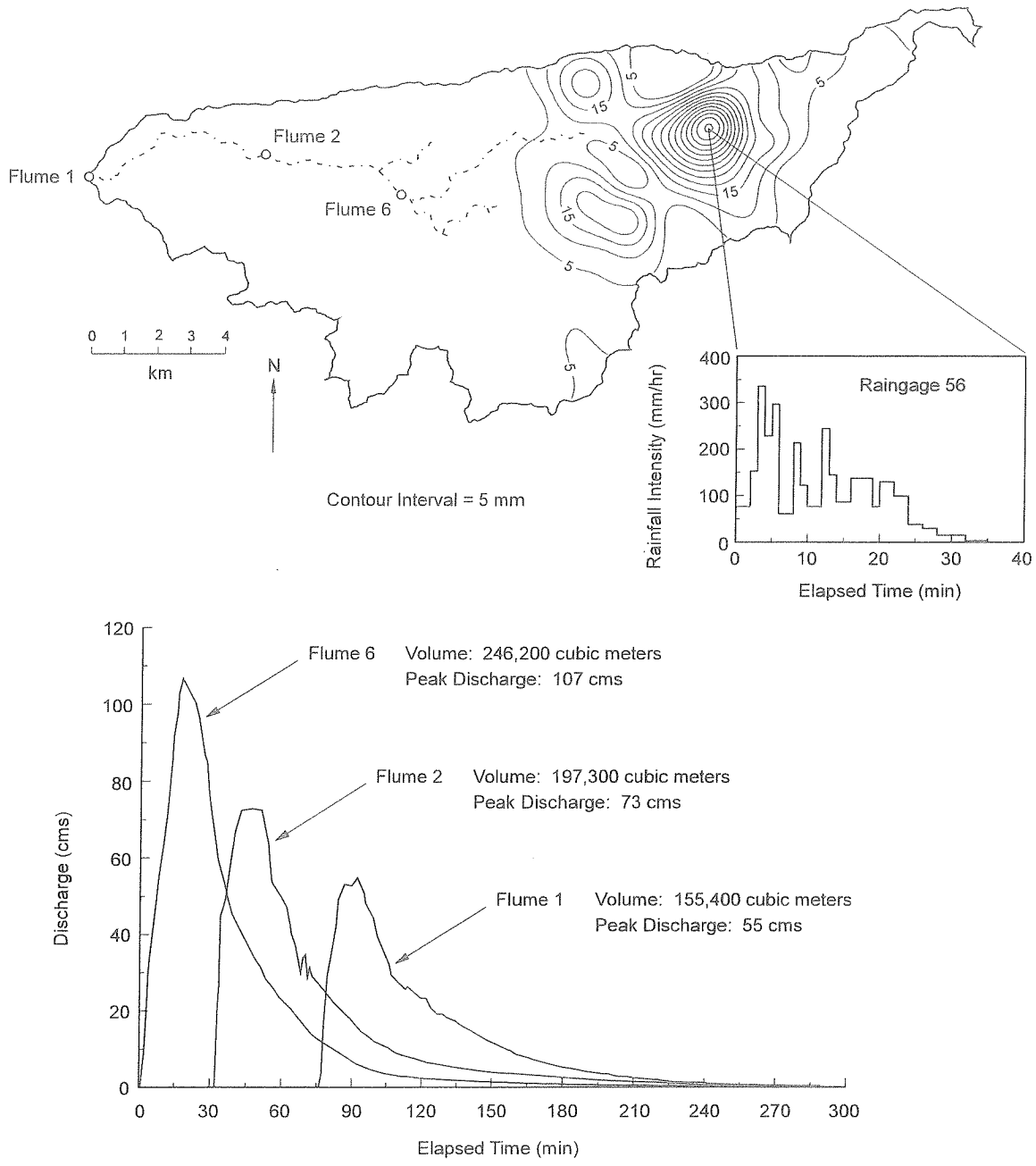

Figure 2. Storm total isohytes and hydrographs from flumes 6, 2, and 1 for event of 27 August 1982.

(1). Ephemeral channel surface areas (Table 1) versus contributing watershed area were plotted as open circles in the upper portion of Figure 3. These data were derived by digitizing polygons of planimetric channel projections from 1:5000 orthophotomaps (Figure 1, inset). A brief description of how these data were obtained and a discussion of potential sources of error in the channel area data are contained in the appendix [also see *Miller et al.*, 1996a, b]. As noted above and illustrated in Figure 2, channel transmission losses have a substantial impact on watershed runoff response in ephemeral drainage systems. Effective channel infiltration rates have been estimated to be 2–10 times greater than upland infiltration rates based on hillslope rainfall simulator studies [*Kincaid et al.*, 1964; *Tromble et al.*, 1974] and analyses of interflume losses from events where lateral channel inflows are insignificant, such as the event illustrated in Figure 2 [*Keppel and Renard*, 1962; *Lane*, 1983; *Unkrich and Osborn*, 1987].

Closer examination of the data presented in the top portion of Figure 3 and in Table 1 reveals that the channel area to mean annual runoff ratio (Table 1) is less than 1 for all but one watershed with drainage areas less than roughly 3.7×10^5 m^2 (37 ha) and is greater than 1 for all watersheds with drainage areas equal to or larger than 37 ha. Below 37 ha the average ratio of channel area to mean annual runoff volume is 0.61, while above this drainage area it is 6.41. Similarly, the average ratio of channel area to drainage area is 0.012 below 37 ha and is 0.046 above 37 ha. This indicates that substantially greater channel area per unit area of drainage area exists for the watersheds larger than roughly 37 ha. Thus larger watersheds have a relatively higher proportion of channel area with

Table 1. Walnut Gulch Watersheds: Drainage Area, 1969–1979 Mean Annual Runoff Volume, Channel Area, Ratio Channel Area to Mean Annual Runoff, and Ratio Channel Area to Drainage Area

Point	Watershed Identification Number	Drainage Area Without Ponds, m^2	Mean Annual Runoff, m^3	Channel Area (m^2)	(Channel Area)/ (Mean Annual Runoff)	(Channel Area)/ (Drainage Area)
1	105	1.821e + 03	28	47	1.72	0.026
2	106	3.440e + 03	89	0	0.00	0.000
3	101	1.295e + 04	307	230	0.75	0.018
4	102	1.457e + 04	297	91	0.31	0.006
5	112	1.862e + 04	269	0	0.00	0.000
6	103	3.683e + 04	824	565	0.69	0.015
7	104	4.533e + 04	818	707	0.86	0.016
8	121	5.423e + 04	1,178	617	0.52	0.011
9	215	3.695e + 05	7,256	10,271	1.42	0.028
10	201	4.411e + 05	7,366	35,995	4.89	0.082
11	223	4.827e + 05	9,111	17,076	1.87	0.035
12	220	6.042e + 05	8,511	12,575	1.48	0.021
13	216	8.967e + 05	8,507	62,461	7.34	0.070
14	208	1.033e + 06	9,292	62,460	6.72	0.060
15	214	1.451e + 06	29,536	39,995	1.35	0.028
16	207	1.516e + 06	8,550	37,982	4.44	0.025
17	213	1.530e + 06	8,211	8,239	1.00	0.005
18	4	2.290e + 06	15,678	150,093	9.57	0.066
19	212	3.570e + 06	25,152	153,867	6.12	0.043
20	3	5.459e + 06	39,389	268,330	6.81	0.049
21	11	6.354e + 06	65,977	391,090	5.93	0.062
22	8	1.326e + 07	103,425	700,055	6.77	0.053
23	7	1.363e + 07	119,586	279,840	2.34	0.021
24	10	1.478e + 07	63,056	610,383	9.68	0.041
25	15	1.640e + 07	88,927	2,305,404	25.92	0.141
26	9	2.076e + 07	188,405	702,952	3.73	0.034
27	6	8.147e + 07	373,051	2,800,555	7.51	0.034
28	2	9.561e + 07	435,977	3,497,769	8.02	0.037
29	1	1.310e + 08	417,914	4,907,226	11.74	0.037

greater effective infiltration rates, which increases the potential for channel transmission losses.

The increased potential for channel transmission losses with increasing drainage area lead to consideration of the potential change in linearity of watershed response [*Huang and Willgoose*, 1993] by examining the behavior of the exponent of (1). A two-segment power law regression in the form of (1) was computed for the mean annual flow to drainage area observations in the top portion of Figure 3. Regressions were developed for both the lower and upper segments by sequentially including more points in the lower regression and fewer points in the upper regression. A common transition point was included for both regression segments, and a minimum of four points was used in each regression. For example, the initial two-segment lower and upper observation set consists of using points 1–4 and 4–29, the second set utilizing points 1–5 and 5–29 of Table 1 and so on. The residual from the two-segment regression was computed according to the following equation and was plotted versus the drainage area of the common point in the lower portion of Figure 3:

$$\text{Residual} = \frac{\sum_{i=1}^{n_1} (\log V_{l,i} - \log V_{o,i})^2}{n_1} + \frac{\sum_{i=n_1}^{n_2} (\log V_{u,i} - \log V_{o,i})^2}{n_2 - n_1 + 1} \quad (3)$$

$$n_1 = 4, 5, \cdots, 26 \quad n_2 = 29$$

where V_l is the lower regression model estimate, V_u is the upper regression model estimate, and V_o is the observed mean annual runoff volume (in cubic meters).

The computed residual is minimized at point 12 (watershed 220), which has a drainage area of 6.0×10^5 m^2 (60 ha). Using point 12 as the break between the lower and upper regression segments, the exponent b of (1) is 0.97 for the lower segment (points 1–12) and 0.82 for the upper segment (points 12–29). In Figure 4 the regression models for the two segments are superimposed on the same mean annual runoff and channel area data as presented in the upper portion of Figure 3. A null hypothesis of equal slopes (exponent b) of the lower and upper segment regressions was rejected at a 95% confidence level. Thus for watershed areas below a transition of drainage areas around 6.0×10^5 m^2 (60 ha) the annual runoff response is nearly linear. Beyond this apparent transition area a much greater degree of basin influence or retardation occurs, as indicated by the significant decrease in the exponent. According to the definition of *Huang and Willgoose* [1993], this implies that watershed runoff response becomes more nonlinear for drainage areas beyond this transition region. Caution should be exercised in trying to define a precise drainage area at which this transition in linearity of watershed response occurs. There are unfortunately no instrumented watersheds on Walnut Gulch in the relatively large region spanned by the drainage areas from 5.4×10^4 to 3.7×10^5 m^2 (5.4–37 ha). In addition to the transition analysis, if weight is given to the change in the ratios of channel area to mean annual runoff and to drainage area noted above, a plausible transition region would span drainage areas from roughly 3.7×10^5 to 6.0×10^5 m^2 (37–60

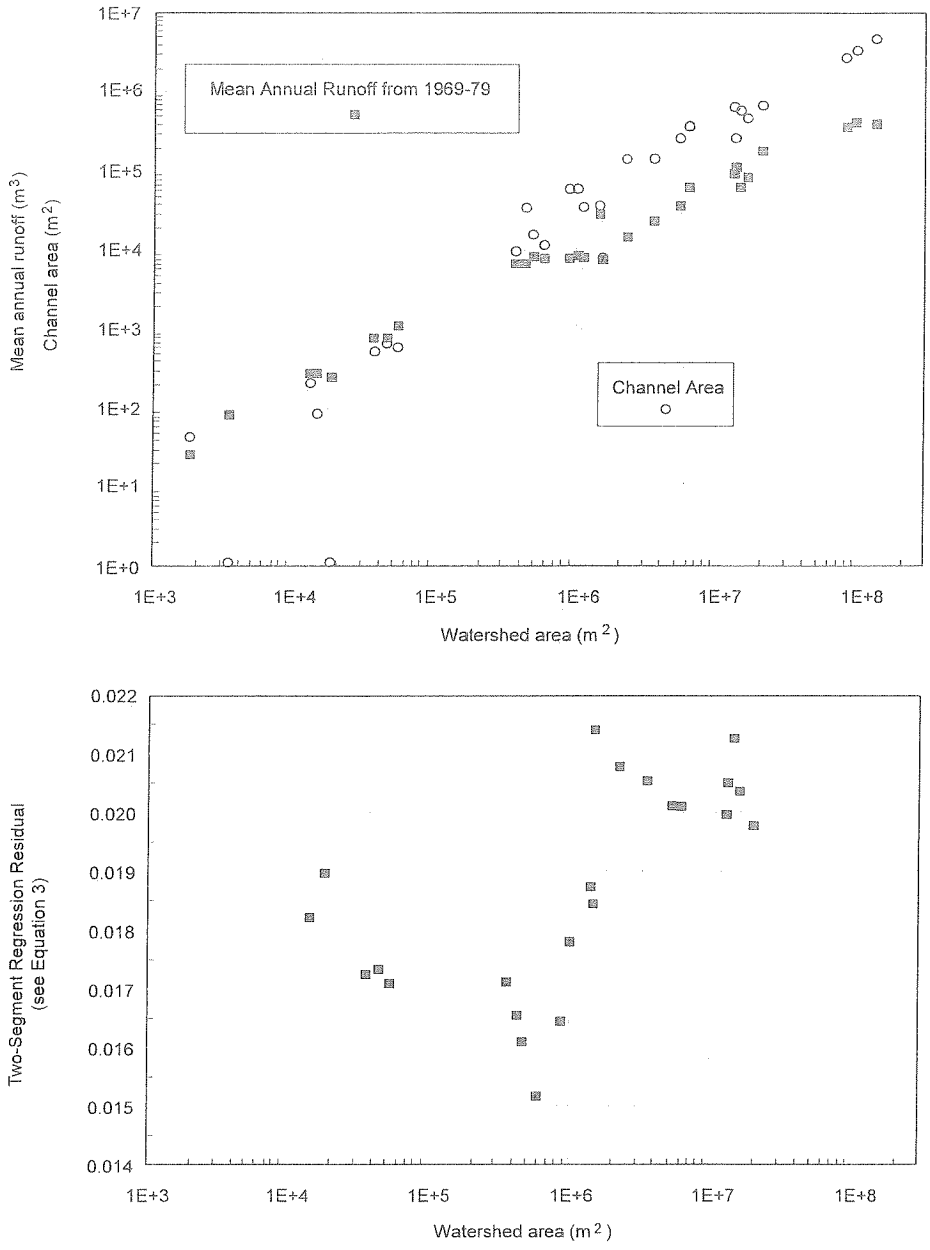

Figure 3. Mean annual runoff volume (solid squares) and, watershed channel area (open circles) as a function of contributing watershed area (top). Two-segment regression residuals (equation (3)) plotted as a function of the drainage area of the common point in the lower and upper regression (bottom).

ha). A wider transition region may very well exist, but it cannot be deduced from the available data set.

Another factor that undoubtedly plays a critical role in runoff generation over a range of watershed scales is partial area storm coverage. This has been noted in a number of studies [e.g., *Gupta and Waymire*, 1993; *Gupta and Dawdy*, 1994, 1995; *Seo and Smith*, 1996a, b; J. B. Marco and J. B. Valdes, Partial area coverage distribution for arid regions flood frequency analysis, unpublished manuscript, 1996] and is clearly illustrated for the single event depicted in Figure 2. In the study region, air mass thunderstorms of limited spatial extent are responsible for virtually all of the runoff production via infiltration excess [*Renard et al.*, 1993]. To understand the properties of partial watershed storm coverage, 304 summer storm events with observations from 91 rain gauges were analyzed. For each storm, observed rainfall totals and accumulations at 10-min intervals during the storm were interpolated onto a 100 × 100 m grid covering Walnut Gulch using multiquadric methods [*Syed*, 1994]. From this data the ratio of total storm area (A_{storm}) coverage to watershed area ($A_{\text{watershed}}$) was computed for 25 of the 26 watersheds. The average storm area with 10-min intensities greater than 25 mm/hr (designated the storm core) was also computed ($A_{\text{storm core}}$). These storm core data were used as a conservative estimate for the portions of the storm generating runoff because large parts of the total storm area have insufficient intensity for runoff generation. This is supported by the results of *Osborn and Laursen* [1973] and *Syed* [1994], who noted a significantly higher correlation between storm core volume and total runoff than the correlation between total storm volume and total runoff. In both

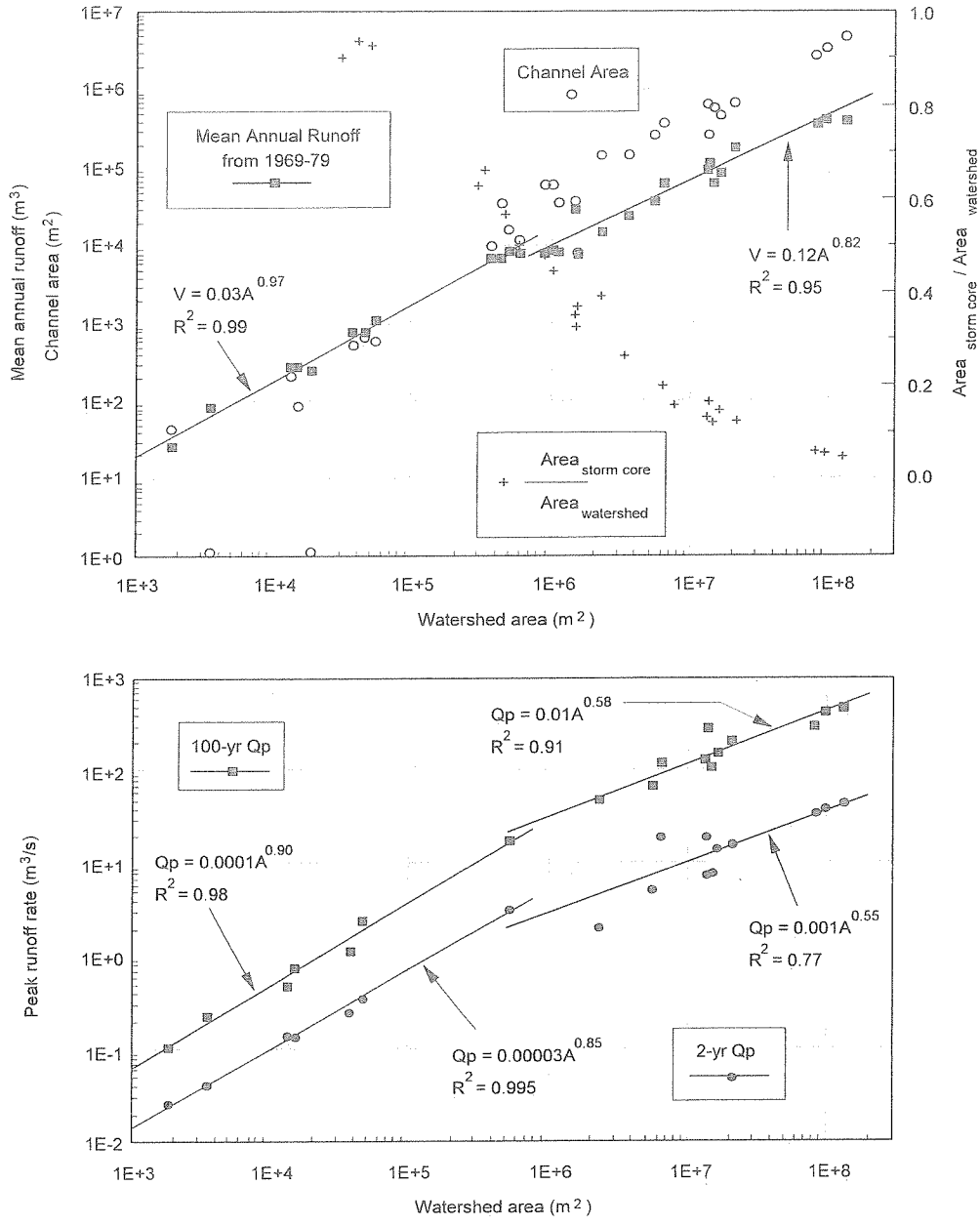

Figure 4. Mean annual runoff volume (solid squares), watershed channel area (open circles), and storm core area to watershed area ratio (crosses) as a function of drainage area and two-segment power law regressions based on the transition break defined by the minimum residual from Figure 3 (top). Database-derived peak runoff rates versus drainage area for 2- and 100-year return periods and two-segment power law regressions based on the transition break defined by the minimum residual from Figure 3 (bottom).

cases, statistics were computed only from storms that had a nonzero storm or storm core area, resulting in a variable number of samples for each watershed. Using data from *Syed* [1994], the mean of the ratios of total storm areas and storm cores to watershed area are plotted in Figure 5.

Note that the total storm area ratio ($A_{storm}/A_{watershed}$) is virtually identical to the storm core ratio ($A_{storm\ core}/A_{watershed}$) for small watershed areas. At larger watershed areas, however, the ($A_{storm}/A_{watershed}$) diverges rapidly from the storm core ratio ($A_{storm\ core}/A_{watershed}$), reaching a factor of 2 greater at roughly 1×10^6 m^2 (100 ha) and increasing to almost 7.5 times greater at the largest watershed area. The variances of these ratios follow similar trends. The storm core to watershed ratio ($A_{storm\ core}/A_{watershed}$) was also computed for the watersheds excluding the stock pond drainage area. These ratio data are plotted as pluses in the top portion of Figure 4. They exhibit a relatively rapid rate of decrease from roughly 3.5×10^4 to 5.5×10^6 m^2 (3.5–550 ha) and a slower of decline beyond 550 ha. This decrease in the percent cover of the storm core further contributes to the decrease in watershed yield and nonlinearity in basin response beyond the transition region.

To investigate the potential changes in peak runoff rate as a function of drainage area, database-derived estimates of the 2- and 100-year peak runoff rates were estimated on the basis of annual peak flow observations from 18 of the 29 watersheds with high-quality peak discharge records for periods of record

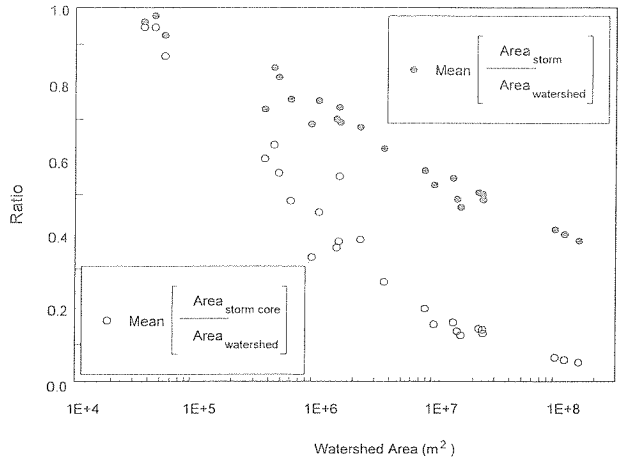

Figure 5. Mean of total storm area (A_{storm}) to watershed area ($A_{\text{watershed}}$) ratio and storm core area ($A_{\text{storm core}}$) to watershed area ratio as a function of watershed area for $A_{\text{storm}} > 0$ and $A_{\text{storm core}} > 0$.

ranging from 15 to 28 years [*Eychaner*, 1984; *Lane*, 1985; *Boughton et al.*, 1987]. The 2- and 100-year peak flow estimates are plotted as solid circles and squares, respectively, in the lower portion of Figure 4. Using the transition region defined by observations and analyses of the mean annual runoff volume noted above, similar two-segment power law regressions were derived for the peak runoff estimates. For these regressions the decrease in exponent d of (2) is much greater than that which was found for the mean annual runoff volume. As in the case for runoff volume a significant decrease (at a 95% confidence level) in the exponent d was observed for both the 2- and 100-year return periods. For the 2-year return period the exponent decreased from 0.85 to 0.55, and for the 100-year return period it decreased from 0.90 to 0.58 (see lower portion of Figure 4). Being analogous to the scale-dependent trends in annual runoff volume and using the definitions of *Huang and Willgoose* [1993], this trend indicates an increasing degree of nonlinearity (greater retardation or filtering effects) in runoff response with increasing watershed scale. However, given the period of record used to estimate the 100-year peak runoff rates, caution must be exercised in interpreting these data.

3. Simple Distributed Modeling for Peak Flow Estimation

This section and the following section describe the use of two distributed hydrologic models with different levels of complexity to further investigate the reasons for, and potential implications of, the observed increase in nonlinearity of runoff response with increasing basin scale indicated by the hydrologic data presented in the previous section. In this section the distributed watershed model developed by *Lane* [1982, 1983] was applied to the entire Walnut Gulch watershed and separately to the 11 largest nested watersheds. The model was used to compute peak runoff rates using depth-area-frequency relationships to obtain rainfall inputs. These relationships are typically used in ungauged watersheds to define runoff model inputs [*Osborn and Renard*, 1988]. This allowed examination of the influence of partial area storm coverage (e.g., Figures 2 and 5) and increasing watershed response nonlinearities (e.g., Figure 4) on the basis of a simple distributed model's ability to simulate peak flow estimates. In this model, runoff volumes from upland and lateral contributing areas to the channel network are computed on the basis of curve number methods [*U.S. Department of Agriculture–Soil Conservation Service (USDA-SCS)*, 1985]. Peak upland and lateral runoff rates are computed on the basis of estimates of mean flow duration and runoff volume. The mean flow duration was estimated using a power law relation based on data from 15 semiarid watersheds in Arizona with 10–35 years of record [*Murphey et al.*, 1977].

Upland and lateral runoff volume and peak rates are input into the channel component of *Lane*'s [1982] model. Lane used an ordinary differential equation to approximate the rate of change in runoff volume with distance as

$$\frac{dV}{dx} = -wc - wkV(x, w) + \frac{V_{\text{LAT}}}{x} \tag{4}$$

where $V(x, w)$ is the outflow volume $[L^3]$, w is the average flow width $[L]$, x is the length of channel reach $[L]$, V_{LAT} is the volume of lateral inflow $[L^3]$, and c is a function of the exponential decay factor k, defined below (equation (6)). To derive the coefficients, *Lane* [1982] assumed that observed inflow-outflow data could be related by regression analysis of the form

$$V(x, w) = \begin{cases} 0 & V_{\text{up}} \le V_o(x, w) \\ a(x, w) + b(x, w)V_{\text{up}} & V_{\text{up}} > V_o(x, w) \end{cases} \tag{5}$$

where $a(x, w)$ and $b(x, w)$ are the regression intercept $[L^3]$ and slope, respectively; $V_o(x, w)$ equals the threshold volume $[L^3]$; and V_{up} is the computed inflow volume $[L^3]$. By letting $x = w = 1$ and defining $a(1, 1) = a$, $b(1, 1) = b$, $c = -ka/(1 - b)$ and by using the equivalence of

$$b(x, w) = e^{-kw} \qquad a(x, w) = \frac{a}{1 - b}[1 - e^{-kwx}], \tag{6}$$

the solution to (4) is

$$V(x, w) = a(x, w) + b(x, w)V_{\text{up}} + \frac{V_{\text{LAT}}}{kwx}[1 - b(x, w)] \tag{7}$$

Solution of this equation also effectively computes channel infiltration losses which are controlled by the coefficients in (6) and (7). The effective channel hydraulic conductivity (Ke) can be related to the intercept coefficient a and the decay factor k [*Lane*, 1983]. On the basis of observations from 14 selected ephemeral reaches of watersheds in Arizona, Texas, and Kansas-Nebraska, Ke ranged from 0.25 to 65 mm/hr. The values of Ke within Walnut Gulch computed by *Lane* [1983] were comparable to independently derived estimates from *Keppel and Renard* [1962]. Peak discharge is then computed using the time average loss rate in the channel reach and the peak discharge from the lateral and inflow hydrograph as

$$Q(x, w) = \frac{1}{D}[a(x, w) - (1 - b(x, w))V_{\text{up}}] + b(x, w)Q_{\text{up}} + \frac{[1 - b(x, w)]}{kw}\frac{Q_{\text{PLAT}}}{x} \tag{8}$$

where Q_{up} is the peak of the computed inflow hydrograph $[L^3/T]$, Q_{PLAT} is the peak of the lateral inflow hydrograph $[L^3/T]$, and D is the mean duration of inflow $[T]$. This model was originally developed using data from Walnut Gulch and

independent verification was carried out using data from experimental watersheds near Safford, Arizona [*Lane*, 1982].

This model was applied to the entire Walnut Gulch watershed and 11 of its nested watersheds. To derive the geometric model elements, Walnut Gulch was discretized into 104 upland and lateral overland flow areas and 45 stream channel segments. Following standard practice for USDA-SCS flood peak estimation, average initial soil moisture conditions were assumed for all the simulations. Depth-area-frequency relationships developed by *Osborn et al.* [1980] and *Osborn and Lane* [1981] from Walnut Gulch data were used to estimate the spatially uniform 60-min rainfall depths for 2- and 100-year return period rainfall events for each of the 12 watersheds. A 60-min event was selected since runoff-producing rainfall events on watersheds the size of Walnut Gulch generally last less than 1 hour and infrequently exceed 70 min [*Osborn and Laursen*, 1973]. As in section 2, estimates of the 2- and 100-year peak runoff rates (Qp) were then derived from the observed annual peak series for each of the 11 watersheds [*Eychaner*, 1984; *Lane*, 1985; *Boughton et al.*, 1987].

For each watershed the depth-area adjusted 2-year, 60-min storm from *Osborn and Lane* [1981] was used for model rainfall input. Manual model calibration was carried out by adjusting the SCS curve number for uplands and the saturated hydraulic conductivity for stream channels through the intercept and decay coefficients of (6) and (7). This was done sequentially from small to large watersheds to fit modeled Qp's to the database-derived 2-year Qp on the 12 gauged watersheds. The 2-year Qp calibration results are illustrated in Figure 6. The average absolute error of the predicted 2-year peak rates scaled by the average of the database-derived 2-year peaks after calibration was 0.10 m^3/s, with a slight tendency for the model to overpredict peaks less than 20 m^3/s. The 100-year, depth-area adjusted 60-min storm was then input into the model calibrated for the 2-year peaks to estimate the 100-year flood peaks on each of the watersheds. These estimates are compared to the database-derived estimates in Figure 7. Model-predicted flood peaks were consistently lower than those derived from the observed annual peak series. The average absolute error of the predicted 100-year peaks scaled by the average of the database-derived 100-year peaks was 0.32 m^3/s. Errors in the predicted peaks ranged from 8 to 71% lower than the database estimates, with no discernable trend as a function of watershed area. On the basis of these results, spatial aver-

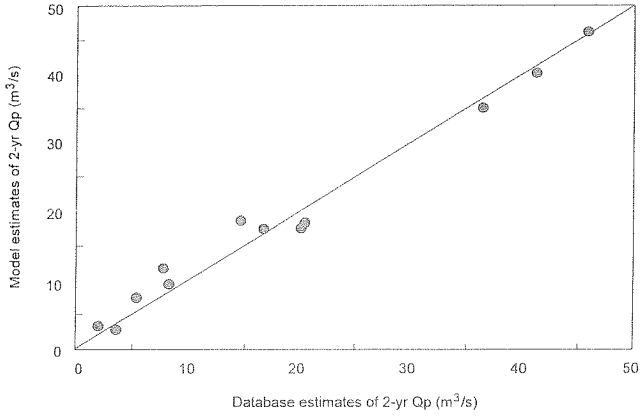

Figure 6. Comparison of model versus database-derived estimates of 2-year peak flows.

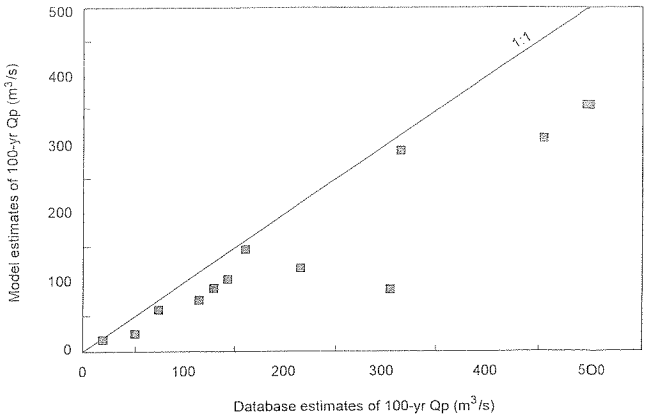

Figure 7. Comparison of model versus database estimates of 100-year peak flow based on calibration using 2-year flows.

aging, or lumping, of rainfall inputs beyond the range of partial area storm coverage illustrated in Figure 5, and inherent in the point-area frequency approach, will result in significant estimation error when used as input into runoff models. Ignoring the within-storm temporal pattern, as was done in this exercise, will also contribute to the under prediction of 100-year peak rates illustrated in Figure 7. Using these lumped inputs to distributed hydrologic models limits their performance in estimating flood peaks. For this reason, further investigation was carried out using a more-complex rainfall-runoff model which explicitly treats temporal and spatial rainfall variability as described in the following section.

4. Detailed Distributed Modeling to Test Basin Response Linearity via the Principle of Proportionality

To further explore the observations noted above, two Lucky Hills watersheds (LH-106 and LH-104) and watershed 11 (WG11; see Figure 1), which span the transition region of drainage areas, were modeled in greater detail with the KINEROS event rainfall-runoff-erosion model [*Woolhiser et al.*, 1990; *Smith et al.*, 1995]. The contributing areas of the three watersheds were discretized into overland flow and channel elements using topographic maps. Geometric, hydraulic, and soil parameters were either measured or estimated for each of the model elements. The infiltration component of this model is based on the *Smith and Parlange* [1978] simplification of Richards' equation [*Jury et al.*, 1991], which assumes a semi-infinite, uniform soil for each model element. The Smith-Parlange model is stated as

$$f_c = K_s \frac{e^{F/B}}{(e^{F/B} - 1)} \qquad B = G\varepsilon(S_{\max} - SI) \tag{9}$$

where f_c is infiltration capacity $[L/T]$; K_s is saturated hydraulic conductivity $[L/T]$; F is infiltrated water $[L]$; B is saturation deficit $[L]$; G is effective net capillary drive $[L]$; ε is porosity; $S_{\max}$ is maximum relative fillable porosity, which is equal to maximum volumetric soil water content divided by ε; and SI is initial relative soil saturation, which is equal to initial volumetric soil water content divided by ε. Runoff generated by infiltration excess is routed interactively using the kinematic wave equations for overland flow and channel flow, respectively stated as

Table 2. Calibration and Verification Coefficient of Efficiencies (Forecast) for Runoff Volume, V, and Peak Rate, Qp

Catchment	Area, m^2	Calibration Efficiency		Verification Efficiency	
		$E(V)$	$E(Qp)$	$E(V)$	$E(Qp)$
LH-106	3.4×10^3	0.98	0.95	0.98	0.79
LH-104	4.4×10^4	0.97	0.98	0.99	0.96
WG-11	6.3×10^6	0.86	0.84	0.49	0.16

$$\frac{\partial h}{\partial t} + \frac{\partial \alpha h^m}{\partial x} = r_i(t) - f_i(x, t)$$
$$\frac{\partial A}{\partial t} + \frac{\partial Q(A)}{\partial x} = q_l(t) + r_i(t) - f_{ci}(x, t) \quad (10)$$

where h is mean overland flow depth $[L]$, t is time, x is distance along the slope $[L]$, $\alpha = 1.49S^{1/2}/n$, S is slope, n is Manning's roughness coefficient, $m = 5/3$, $r_i(t)$ is the rainfall rate $[L/T]$, $f_i(x, t)$ is the infiltration rate $[L/T]$, A is channel cross-sectional area of flow $[L^2]$, $Q(A)$ is channel discharge as a function of area $[L^3/T]$; $q_l(t)$ is net lateral inflow per unit length of channel $[L^2/T]$, $r_i(t)$ is net rainfall per unit length of channel $[L^2/T]$, and $f_{ci}(x, t)$ is net channel infiltration per unit length of channel computed using (9) $[L^2/T]$. These equations are solved using a four-point implicit finite difference method (see *Smith et al.* [1995] for details).

Interactive routing implies that infiltration and runoff are computed at each finite difference node using rainfall, upstream inflow, and current degree of soil saturation. Unlike an excess routing scheme, infiltration can therefore continue after rainfall ceases, given that there is upstream inflow. The model employs a space-time rainfall interpolation method which enables utilization of breakpoint rainfall data from the dense Walnut Gulch rain gauge network. Small-scale variability of infiltration is represented in the model by assuming that the saturated hydraulic conductivity (Ks) within an overland flow element varies lognormally [*Woolhiser and Goodrich*, 1988]. Using this option, the mean Ks and its coefficient of variation (CV_{Ks}) are required for inputs to each overland flow element. These inputs were estimated on the basis of soil texture from soil samples and channel surveys in LH-106 and LH-104 [*Rawls et al.*, 1982; *Woolhiser et al.*, 1990, Table 2] and from soil maps and channel surveys in WG11 [*Goodrich*, 1990].

The model was calibrated using 10 rainfall-runoff events for each of the three watersheds by adjusting three parameters: global multipliers of Manning's roughness (n), Ks, and CV_{Ks}. The multipliers on Manning's roughness and Ks also adjusted n and Ks for the channel elements. Adjusting these multipliers scales these model element input parameters while maintaining relative differences based on field observations. By using this approach, the overall dimension of the adjustable parameter space remains small, at three, which aided in precluding parameter identifiability problems as noted by *Beven* [1989]. Approximately 20 additional events for each of the three watersheds were withheld for split-sample verification. Results were evaluated using *Nash and Sutcliffe* [1970] forecast coefficient of efficiency for runoff volume and peak rate (see Table 2). The coefficient of efficiency (E) was selected because it is dimensionless and easily interpreted. If the model predicts observed runoff volume or peak runoff rate with perfection, $E = 1$. If $E < 0$, then the model's predictive power is worse than simply using the average of observed values.

As judged by the efficiency statistics, the model provides remarkably good predictions of runoff volume and peak response for the Lucky Hills watersheds, LH-106 and LH-104. On WG11 the model performed reasonably well for the calibration event set, but the efficiency statistics dropped off considerably for the verification event set. For the verification set on WG11 the model tended to overestimate the large events and underestimate the small events. This apparent bias was not present in the calibration set for peak or volume. However, the results were still quite good when compared to other modeling efforts on Walnut Gulch [*Hughes and Beater*, 1989] and on other experimental watersheds [*Loague and Freeze*, 1985]. It was assumed that the model results were acceptable for subsequent analysis and that the model provided an adequate representation of the hydrologic response. Therefore it may be utilized to further explore issues of runoff response linearity. Impacts in subsequent analysis from the drop off in model performance for WG11 were mitigated by carrying out sensitivity analysis on the calibration event sets. Using the calibration event set did not impact subsequent interpretation regarding linearity of watershed response because the sensitivity and proportionality results were all judged on the basis of relative changes from the final model predictions.

To address the classical definition of input-output linearity via proportionality and superposition, model sensitivity to perturbations in rainfall was assessed. This was accomplished by scaling the input rainfall distribution by ±15% for each watershed's calibration event set. This approach is consistent with typical rain gauge catch errors reported by *Neff* [1977] and *Hanson* [1989]. The rainfall interpolation algorithm scales the intensities of each rain gauge before spatial interpolation occurs. In so doing the relative scaling in both space and time is preserved throughout the event. This represents a more realistic assessment of model response than an excess approach with uniform rainfall. For this study, total observed rainfall was scaled (not excess rainfall) to allow comparison of the total watershed response across a range of scales. By doing so the impacts of both abstractions (infiltration, interception, and detention storage) and routing on the nature of total watershed runoff response were assessed. If runoff response from the perturbed input exhibits 15% perturbations, watershed response would be linear. The larger the departure from ±15%, the greater the nonlinearity in total watershed response. The runoff perturbations in percent volume change are plotted in Figure 8. Note that the abscissa used for this figure is the observed volume of the runoff event in depth per unit watershed area (in millimeters), thus providing a measure of the relative magnitude of the runoff event.

Examination of Figure 8 reveals that linearity in runoff response would appear not to increase with increasing basin scale, as concluded in a number of prior studies [*Anderson et al.*, 1981; *Dooge*, 1981; *Beven et al.*, 1988; *Wang et al.*, 1981; *Gupta et al.*, 1986]. On the basis of the three watersheds it could be argued that response becomes more nonlinear with increasing watershed scale. Increasing nonlinearity of runoff response also occurs for decreasing event size as the relative runoff perturbations increase for smaller events on Figure 8. This underscores greater relative role or domination of watershed characteristics in retarding or filtering the runoff response with decreasing storm size or increasing watershed scale.

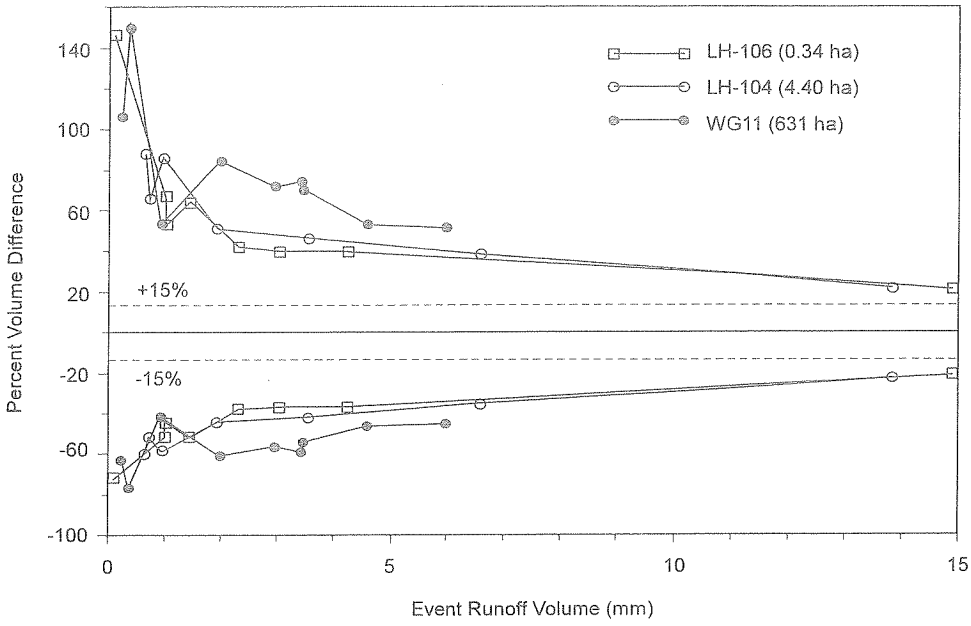

Figure 8. Percent volume difference in modeled runoff volume for a ±15% perturbation in observed rainfall input.

The processes responsible for increasing watershed domination are illustrated by plotting the integrated fluxes of overland and channel infiltration over all watershed model elements together with watershed hyetographs and hydrographs for two events with nearly equal total runoff volume per unit area for LH-104 and WG11 (see Figure 9). The ratio of peak channel infiltration to peak runoff rate is approximately 0.7 for the WG11 event and only 0.02 for the LH-104 event. This illustrates the increasing dominance of channel transmission losses with increasing watershed scale in this environment [*Renard et al.*, 1993; *Boughton and Stone*, 1985]. Additional differential perturbations of overland and channel saturated hydraulic conductivity and roughness, though not shown, further confirmed this trend.

To differentiate between the relative contributions of routing and abstractions (only infiltration in this case) to the nonlinearity of runoff response, a set of simulations was performed on impervious (overland and channel elements) and infiltrating geometries of the three watersheds. For this set of simulations a perturbation of −15% was applied to the rainfall

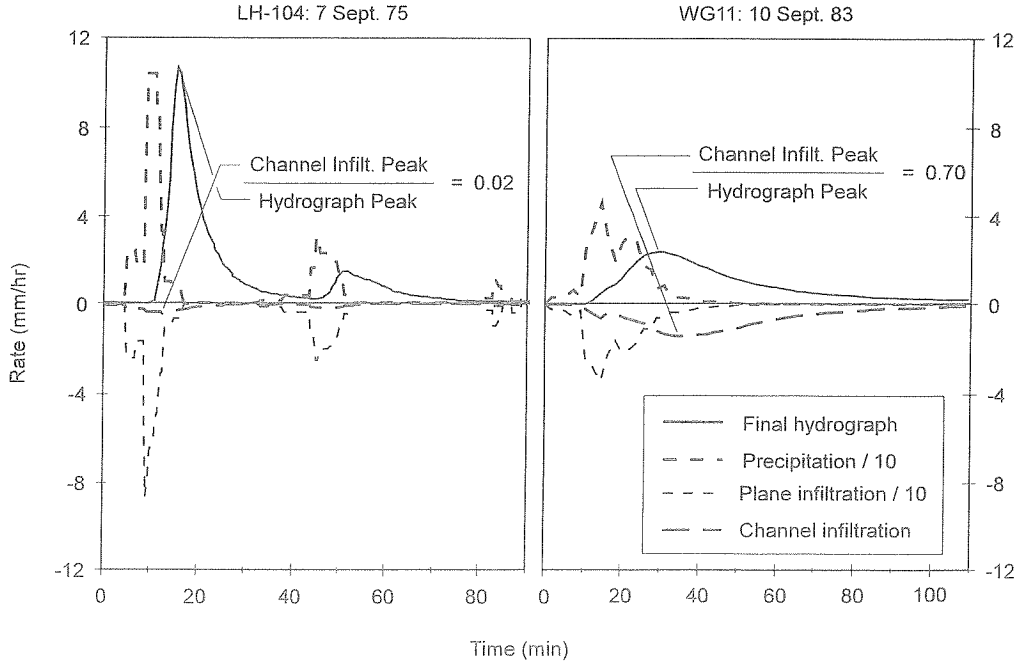

Figure 9. Spatially integrated precipitation, watershed runoff, and overland and channel infiltration fluxes for LH-104 and WG11 with infiltration fluxes plotted as negative values.

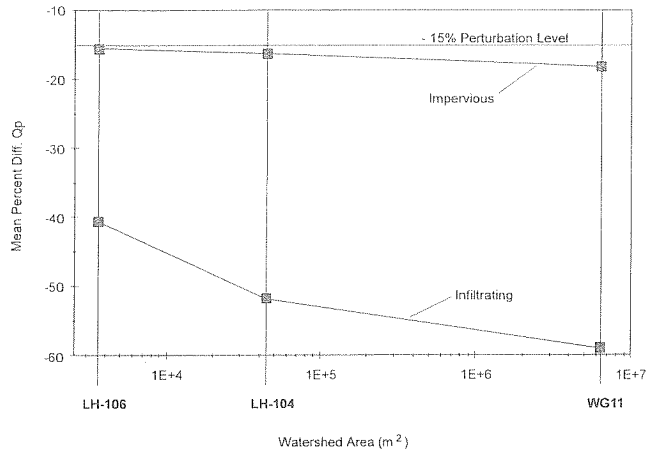

Figure 10. Mean percent change in peak discharge resulting from a −15% decrease in rainfall for impervious and infiltrating cases.

inputs for the calibration events set consisting of 10 events for each watershed. The mean percentage difference of Qp from the unperturbed to perturbed cases is illustrated in Figure 10. It can be seen that a slight increase in response nonlinearity occurs with increasing scale for the impervious case, which is attributed to routing effects. This is not surprising, as the kinematic routing equations used in the model are nonlinear. However, routing effects are far exceeded by infiltration effects which increase with watershed scale. This further illustrates the significance of the observations plotted in Figure 4, which illustrate a decrease in the rate of annual watershed yield and peak runoff rates with increasing drainage area due to the increasing influence of infiltration and transmission loss abstractions. Also note that the relative change from LH-104 to WG11 is less than the change from LH-106 to LH-104. This is due to the fact that the −15% perturbation to the rainfall field has less overall impact on WG11 since the fraction of watershed storm coverage is substantially smaller for WG11 (see Figure 5). The mean fractional coverages of LH-106 and LH-104, which are nested (see Figure 1), are nearly identical and nearly equal to 1, while the mean fraction of WG11 cover by total storm rainfall is 0.56.

5. Discussion and Conclusions

The results from section 4, first presented by *Goodrich* [1990], with the observations and analyses in sections 2 and 3, support the conclusion that watershed runoff response becomes more nonlinear with increasing watershed scale in the semiarid Walnut Gulch watershed. This characteristic of the runoff response is attributed to a threshold associated with channel transmission losses and the continual decrease in the fractional coverage of storm rainfall. *Simanton et al.* [1996] also noted that channel infiltration and spatial rainfall variability were the primary reasons why runoff curve numbers computed from rainfall-runoff observations decreased as watershed size increased. The transition region of drainage area identified in section 2 (roughly $3.7–6.0 \times 10^5$ m^2, or 37–60 ha, but possibly wider) could be interpreted as the range of drainage areas over which a transition occurs from where watershed response is dominated by hillslope processes and channel processes are of secondary importance, to watersheds where hillslope and channel processes are critical for describing runoff response. The relative volumes of water abstracted from overland and channel infiltration illustrated in Figure 9 from the KINEROS analysis for watersheds on either side of the transition region attest to the substantial increase in the role of channel processes in overall runoff response. Associated with the increasing role of channel processes are the nonlinearities inherent in channel infiltration and transmission losses.

As noted in the introduction, *Huang and Willgoose* [1993] strongly argue that the exponents b and d of (1) and (2) are independent of watershed scale and that the values are strongly influenced by watershed retardation and diffusive effects as well as the watershed geomorphology. It should be noted that their study did not treat channel transmission losses or spatially variable rainfall. Observations presented in section 2 indicate that the exponents do change with watershed scale. Watershed retardation in the form of channel transmission losses due to the relative increase in channel area, along with the continual decrease in fractional storm coverage, offers compelling physical evidence to explain changes in the exponents in the critical transition region identified in section 2.

Similarly, *Gupta and Dawdy* [1995] proposed that a critical drainage area exists above which the processes controlling runoff response change. They postulated that flood variability in watersheds larger than the critical area is determined by precipitation input, and for smaller areas it is determined by watershed factors. However, the current investigation implies that the flood response for watersheds larger than the critical threshold is not simply a function of the rainfall input and hillslope runoff generation. The influence of watershed network factors in Walnut Gulch persists because of channel transmission losses or "watershed retardation effects" [*Huang and Willgoose*, 1993]. The transitional range of drainage areas noted above (37–60 ha) is similar in size to the 100-ha representative elementary area (REA) found by *Wood et al.* [1990], although it was not interpreted in the same fashion in this study. The REA denotes the area at which variability in watershed runoff generation largely disappears. The transitional area described in the current study denotes a range of drainage areas over which a relative change in process domination occurs.

Robinson et al. [1995] note that a definitive threshold watershed size above which network response dominates does not exist for their test watersheds in New Zealand. For large watersheds they conclude that modeling watershed storm response should focus on where runoff is generated, with less emphasis placed on rigorous routing through the stream network, as dispersion by channel routing is not important. In semiarid watersheds with ephemeral channels the location of runoff generation is also very important, but rigorous channel routing cannot be ignored. In such an environment, proper routing treatment is critical as it largely determines the channel infiltration opportunity time and area over which transmission losses occur. This requires coupled routing and channel infiltration algorithms.

The reason that increasing nonlinearity of runoff response with increasing scale has not been previously observed may be that effluent streams (runoff per unit area increases with increasing basin size, e.g., gaining streams) in humid environments are much more widely studied. These watersheds often have large, highly damped base and throughflow runoff components that are not observed in the semiarid Walnut Gulch watershed. This study does not preclude the possibility that at watershed scales larger than those studied here, the runoff

response will become more linear as basin size increases. However, it is the opinion of the authors that such a relationship is doubtful in a losing watershed characterized by influent streams.

For conditions represented by those of the Walnut Gulch Experimental Watershed, the following conclusions are drawn from this study:

1. Watershed runoff response becomes more nonlinear with increasing watershed scale, with a critical transition threshold area occurring roughly around 37–60 ha.

2. The primary causes of increasingly nonlinear response are (1) the increasing role of ephemeral channel transmission losses and (2) the continual decline of fractional storm area coverage.

3. Significant error will result in runoff model estimates of peak discharge when rainfall inputs from depth area-frequency relationships are applied beyond the area of typical storm coverage.

4. For runoff modeling purposes, explicit treatment of channel routing and infiltration will be required for watersheds larger than the transition area.

Although these conclusions are based on total rainfall and runoff versus effective rainfall and direct runoff, they indicate that the application of analyses based on the assumption of linear runoff response in semiarid regions, such as unit hydrograph–based approaches, may be inappropriate. The limited spatial uniformity of rainfall in semiarid regions, even at the scale of 100–300 m [*Goodrich et al.*, 1995; *Faurès et al.*, 1995], in combination with increasing nonlinearities associated with channel losses would limit applications of unit hydrographs (UH) to small watersheds. However, the inappropriateness of UH concepts on small watersheds has been clearly demonstrated by *Minshall* [1960]. Thus small watershed response starts out responding in a highly nonlinear manner and becomes more nonlinear as scales increase for semiarid regions represented by Walnut Gulch. However, direct testing of UH methods in arid or semiarid regions over a range of watershed scales will be required to fully verify this assertion.

Pilgrim et al. [1988] conclude that the distinctive features of arid and semiarid regions may require modeling approaches that differ from humid regions. Certainly, the explicit treatment and modeling of channel transmission losses is required. The increase in nonlinearity with watershed size also makes it more difficult to formulate response relationships at the watershed scale [*Dooge*, 1986]. Both position and timing of water movement are important not only for initial runoff generation but also along the runoff pathway to the watershed outlet due to potential reinfiltration through channel losses.

Appendix

Channel area data were derived from 1:5000 orthophotomaps obtained from low-level aerial photography (1:12,000 average photo scale) and analytic photogrammetric mapping techniques. These maps meet or exceed national map accuracy standards. The channel data were derived by digitizing polygons of planimetric channel projections from the 1:5000 orthophotomaps. Incised channel, swale, and dry pond areas were included in the derivation of total ephemeral channel area as a function of watershed drainage area since they represent areas over which enhanced runoff transmission losses can occur. The areas of incised channels, upland swales, and dry ponds behind impoundments were digitized and imported into a geographic information system (GIS). The channel boundaries of incised drainages with widths of approximately 1 m were discernable on the orthophoto maps. By using GIS techniques, the total channel surface area for channels wider than 1 m were determined. For first-order channels where the width was not clearly visible, a width of 0.5 m was assumed. Swales were identified on the basis of cross-channel slope breaks and a transition of vegetation type and density from the swales to lateral hillslopes [*Miller et al.*, 1996a, b]. The orthophoto base from which the stream channels were delineated was of high quality, allowing for detailed articulation of the stream channels within the GIS. Potential sources of error exist in this method, however, and these errors could impact the estimation of channel surface area: (1) the channel edges were transcribed by hand from the photo base onto a mylar base, allowing for human error; (2) the digitizing process introduces some variation in the channel edge location; (3) the selection of 0.5 m as the mean channel width of first-order channels is somewhat arbitrary and is a potential source of either overestimation or underestimation of surface area. Digitizing errors will either artificially widen or narrow the resultant stream channels, and these errors will largely cancel each other out throughout the process of digitizing the entire channel network. Any such errors would furthermore tend to be repeated throughout the channel network and would therefore not artificially impose an abrupt change in the channel area as a function of drainage area.

Acknowledgments. This study would not have been possible without the dedication of the USDA-ARS Southwest Watershed Research Center, which provided financial support in development and maintenance of the Walnut Gulch Experimental Watershed research facilities and diligent long-term collection of high quality hydrologic data. Special thanks are extended to the staff located in Tombstone, Arizona, for their continued efforts. Support for this effort was provided by USDA-ARS, and in part by the NASA/EOS grant NAGW2425. Financial assistance during the course of graduate work of the senior author, when much of the analysis presented in section 4 was completed, was provided by the National Science Foundation via a Graduate Research Fellowship, the American Society of Civil Engineers and the Hydrology Section of the American Geophysical Union for research fellowships, the U.S. Geological Survey, and the U.S. Department of Energy (Los Alamos National Laboratory). This assistance is gratefully acknowledged. The authors would also like to thank Kevin Lansey, Roger Simanton, Jurgen Garbrecht, Ken Potter, Don Davis, Jens Refsgaard, Carl Unkrich, and two anonymous reviewers for thorough reviews and helpful suggestions.

References

Alexander, G. N., Effect of catchment area on flood magnitude, *J. Hydrol.*, *16*, 225–240, 1972.

Anderson, M. G., D. Boswroth, and P. E. Kneale, Controls on overland flow generation, in *Catchment Experiments in Fluvial Geomorphology*, edited by T. P. Burt and D. E. Walling, pp. 21–34, Geo Books, Norwich, Conn., 1981.

Benson, M. A., Factors influencing the occurrence of floods in a humid region of diverse terrain, *U.S. Geol. Surv. Water Supply Pap. 1580-B*, 64 pp., 1962.

Benson, M. A., Factors affecting the occurrence of floods in the Southwest, *U.S. Geol. Surv. Water Supply Pap. 1580-D*, 72 pp., 1964.

Beven, K. J., Changing ideas in hydrology—the case of physically-based models, *J. Hydrol.*, *105*, 157–172, 1989.

Beven, K. J., E. F. Wood, and M. Sivapalan, On hydrological heterogeneity-catchment morphology and catchment response, *J. Hydrol.*, *100*, 353–375, 1988.

Boughton, W. C., and J. J. Stone, Variation of runoff with watershed area in a semiarid location, *J. Arid Environ.*, *9*, 13–25, 1985.

Boughton, W. C., K. G. Renard, and J. J. Stone, Flood frequency

estimates in southeastern Arizona, *J. Irrig. Drain. Eng.*, *113*(ID4), 469–478, 1987.
Chow, V. T., *Handbook of Applied Hydrology*, pp. 14–34, McGraw-Hill, New York, 1964.
Dooge, J. C. I., A general theory of the unit hydrograph, *J. Geophys. Res.*, *64*(2), 214–256, 1959.
Dooge, J. C. I., Parameterization of hydrologic processes, in *Land Surface Processes in Atmospheric General Circulation Models*, edited by P. S. Eagleson, pp. 243–288, Cambridge Univ. Press, New York, 1982.
Dooge, J. C. I., Looking for hydrologic laws, *Water Resour. Res.*, *22*(9), 46S–58S, 1986.
Eychaner, J. H., Estimation of magnitude and frequency of floods in Pima County, Arizona, with comparisons of alternative methods, *U.S. Geol. Surv. Water Resour. Invest. Rep. 84-4142*, 69 pp., 1984.
Faurès, J. M., D. C. Goodrich, D. A. Woolhiser, and S. Sorooshian, Impact of small-scale spatial rainfall variability on runoff simulation, *J. Hydrol.*, *173*(1995), 309–326, 1995.
Goodrich, D. C., Geometric simplification of a distributed rainfall-runoff model over a range of basin scales, Ph.D. dissertation, 361 pp., Univ. of Ariz., Tucson, 1990.
Goodrich, D. C., J. M. Faurès, D. A. Woolhiser, L. J. Lane, and S. Sorooshian, Measurement and analysis of small-scale convective storm rainfall variability, *J. Hydrol.*, *173*(1995), 283–308, 1995.
Gupta, V. K., and D. R. Dawdy, Regional analysis of flood peaks: Multiscaling theory and its physical basis, in *Advances in Distributed Hydrology*, edited by R. Russo, A. Peano, I. Becchi, and G. A. Bemporad, pp. 149–168, Water Resour. Publ., Littleton, Colo., 1994.
Gupta, V. K., and D. R. Dawdy, Physical interpretations of regional variations in the scaling exponents of flood quantiles, in *Scale Issues in Hydrological Modeling*, edited by J. D. Kalma and M. Sivapalan, pp. 105–119, John Wiley, New York, 1995.
Gupta, V. K., and E. C. Waymire, Statistical self-similarity in river networks parameterized by elevation, *Water Resour. Res.*, *25*(3), 463–476, 1989.
Gupta, V. K., and E. C. Waymire, A statistical analysis of mesoscale rainfall as a random cascade, *J. Appl. Meteorol.*, *32*(2), 251–267, 1993.
Gupta, V. K., E. C. Waymire, and I. Rodriguez-Iturbe, On scales, gravity and network structure in basin runoff, in *Scale Problems in Hydrology*, edited by I. Rodriguez-Iturbe, V. K. Gupta, and E. F. Wood, chap. 8, D. Reidel, Norwell, Mass., 1986.
Gwinn, W. R., The Walnut Gulch supercritical flumes, *J. Hydraul. Div. Am. Soc. Civ. Eng.*, *98*(HY8), 1681–1689, 1970.
Hanson, C. L., Precipitation catch measured by the Wyoming shield and the dual-gauge system, *Water Resour. Bull.*, *25*(1), 159–164, 1989.
Huang, H. Q., and G. Willgoose, Flood frequency relationships dependent on catchment area: An investigation of causal relationships, paper presented at Towards the 21st Century, Engineering for Water Resources Conference, Inst. of Eng.–Aust., Newcastle, Australia, June 30, 1993.
Hughes, D. A., and A. B. Beater, The applicability of two single event models to catchments with different physical characteristics, *Hydrol. Sci. J.*, *34*(1/2), 63–78, 1989.
Jury, W. A., W. R. Gardner, and W. H. Gradner, *Soil Physics*, pp. 105–107, John Wiley, New York, 1991.
Keppel, R. V., and K. G. Renard, Transmission losses in ephemeral stream beds, *J. Hydraul. Div. Am. Soc. Civ. Eng.*, *88*(HY3), 59–68, 1962.
Kincaid, D. R., J. L. Gardner, and H. A. Schreiber, Soil and vegetation parameters affecting infiltration under semiarid conditions, *Bull. IASH*, *65*, 440–453, 1964.
Lane, L. J., Distributed model for small semiarid watersheds, *J. Hydraul. Div. Am. Soc. Civ. Eng.*, *108*(HY10), 1114–1131, 1982.
Lane, L. J., Transmission losses, in *SCS National Engineering Handbook*, Chap. 19, pp. 19-1–19-21, U.S. Govt. Print. Off., Washington, D. C., 1983.
Lane, L. J., Estimating transmission losses, paper presented at Specialty Conference on Development and Management Aspects of Irrigation and Drainage Systems, Irrig. and Drain. Div., Am. Soc. Civ. Eng., San Antonio, Tex., 1985.
Leopold, L. B., M. G. Wolman, and J. P. Miller, *Fluvial Processes in Geomorphology*, W. H. Freeman, San Francisco, Calif., 1964.
Loague, K. M., and R. A. Freeze, A comparison of rainfall runoff modeling techniques on small upland catchments, *Water Resour. Res.*, *21*(2), 229–248, 1985.
Maidment, D. R. (Ed.), *Handbook of Hydrology*, p. 9.26, McGraw-Hill, New York, 1992.
Miller, S. N., D. P. Guertin, and D. C. Goodrich, Investigating stream channel morphology using a geographic information system, paper presented at User Conference, Environ. Syst. Res. Inst., Redlands, Calif., May 20–24, 1996a. (Available as http://www.esri.com/base/common/userconf/proc96/TO300/PAP291/P291.HTM)
Miller, S. N., D. P. Guertin, and D. C. Goodrich, Linking GIS and geomorphologic field research at Walnut Gulch Experimental Watershed, paper presented at 32nd Annual Conference and Symposium: GIS and Water Resources, Am. Water Resour. Assoc., Ft. Lauderdale, Fla., Sept. 22–26, 1996b.
Minshall, N. E., Predicting storm runoff on small experimental watersheds, *J. Hydraul. Div. Am. Soc. Civ. Eng.*, *86*(HYB), 17–38, 1960.
Murphey, J. B., D. E. Wallace, and L. J. Lane, Geomorphic parameters predict hydrograph characteristics in the Southwest, *Water Resour. Bull.*, *13*(1), 25–38, 1977.
Nash, J. E., and J. V. Sutcliffe, River flow forecasting through conceptual models, I, A discussion of principles, *J. Hydrol.*, *10*, 228–290, 1970.
Neff, E. L., How much rain does a raingage gage?, *J. Hydrol.*, *35*, 213–220, 1977.
Osborn, H. B., and L. J. Lane, Point-area-frequency conversions for summer rainfall in southeastern Arizona, paper presented at 1981 Meetings of the Arizona Section–American Water Resources Association and the Hydrology Section–Arizona-Nevada Academy of Science, Tucson, Ariz., May 1–2, 1981.
Osborn, H. B., and E. M. Laursen, Thunderstorm Runoff in Southeastern Arizona, *J. Hydraul. Div., Am. Soc. Civ. Eng.*, *99*(HY7), 129–1145, 1973.
Osborn, H. B., and K. G. Renard, Rainfall intensities for southeastern Arizona, *J. Irrig. Drain. Eng.*, *114*(ID1), 195–199, 1988.
Osborn, H. B., L. J. Lane, and V. A. Myers, Rainfall/watershed relationships for southwestern thunderstorms, *Trans. Am. Soc. Civ. Eng.*, *23*(1), 82–87, 91, 1980.
Pilgrim, D. H., T. G. Chapman, and D. G. Doran, Problem of rainfall-runoff modeling in arid and semiarid regions, *Hydrol. Sci. J.*, *33*(4), 379–399, 1988.
Rawls, W. J., D. L. Brakensiek, and K. E. Saxton, Estimation of soil water properties, *Trans. Am. Soc. Agric. Eng.*, *25SW*, 1316–1320, 1328, 1982.
Renard, K. G., L. J. Lane, J. R. Simanton, W. E. Emmerich, J. J. Stone, M. A. Weltz, D. C. Goodrich, and D. S. Yakowitz, Agricultural impacts in an arid environment: Walnut Gulch case study, *Hydrol. Sci. Technol.*, *9*(1–4), 145–190, 1993.
Robinson, J. S., M. Sivapalan, and J. D. Snell, On the relative roles of hillslope processes, channel routing, and network geomorphology in the hydrologic response of natural catchments, *Water Resour. Res.*, *31*(12), 3089–3101, 1995.
Rodriguez-Iturbe, I., and J. B. Valdes, The geomorphologic structure of hydrologic response, *Water Resour. Res.*, *15*(6), 1409–1420, 1979.
Seo, D. J., and J. A. Smith, On the relationship between catchment scale and climatological variability of surface runoff volume, *Water Resour. Res.*, *32*(3), 633–643, 1996a.
Seo, D. J., and J. A. Smith, Characterization of the climatological variability of mean areal rainfall through fractional coverage, *Water Resour. Res.*, *32*(7), 2087–2095, 1996b.
Simanton, J. R., R. H. Hawkins, M. Mohseni-Sarvai, and K. G. Renard, Runoff curve number variation with drainage area, Walnut Gulch, Arizona, *Trans. Am. Soc. Civ. Eng.*, *39*(4), 1391–1394, 1996.
Smith, R. E., and J.-Y. Parlange, A parameter-efficient hydrologic infiltration model, *Water Resour. Res.*, *14*(33), 533–538, 1978.
Smith, R. E., D. L. Chery Jr., K. G. Renard, and W. R. Gwinn, Supercritical flow flumes for measuring sediment-laden flow, *Tech. Bull. U.S. Dep. Agric.*, *1655*, 70 pp., 1982.
Smith, R. E., D. C. Goodrich, D. A. Woolhiser, and C. L. Unkrich, KINEROS—A kinematic runoff and erosion model, in *Computer Models of Watershed Hydrology*, edited by V. J. Singh, chap. 20, pp. 697–732, Water Resour. Publ., Highlands Ranch, Colo., 1995.
Syed, K. H., Spatial storm characteristics and basin response, M.S. Thesis, 261 pp., Univ. of Ariz., Tucson, 1994.
Tromble, J. M., K. G. Renard, and A. P. Thatcher, Infiltration for three rangeland soil-vegetation complexes, *J. Range Manage.*, *27*(4), 318–321, 1974.

U.S. Department of Agriculture–Agricultural Research Service, Linear theory of hydrologic systems, *Tech. Bull. U.S. Dep. Agric., 1468*, 327 pp., 1973.

U.S. Department of Agriculture–Soil Conservation Service, *National Engineering Handbook*, sect. 4, Hydrology (revised), pp. 19-1–19-21, Washington, D. C., 1985.

Unkrich, C. L., and H. B. Osborn, Apparent abstraction rates in ephemeral channels: Hydrology and Water Resources in Arizona and the Southwest, paper presented at 1987 Meetings of Arizona Section–American Water Resources Association, Hydrology Section–Arizona-Nevada Academy of Sciences, and the Arizona Hydrological Society, Flagstaff, Ariz., April 18, 1987.

Wang, C. T., V. K. Gupta, and E. Waymire, A geomorphologic synthesis of nonlinearity in surface runoff, *Water Resour. Res., 17*(3), 545–554, 1981.

Wood, E. F., M. Sivapalan, and K. J. Beven, Similarity and scale in catchment storm response, *Rev. Geophys., 28*, 1–18, 1990.

Woolhiser, D. A., and D. C. Goodrich, Effect of storm rainfall intensity patterns on surface runoff, *J. Hydrol., 102*, 335–354, 1988.

Woolhiser, D. A., R. E. Smith, and D. C. Goodrich, KINEROS—A kinematic runoff and erosion model: Documentation and user manual, *U.S. Dep. Agric. Agric. Res. Serv. Publ. ARS-77*, 130 pp., 1990.

D. C. Goodrich, L. J. Lane, S. N. Miller, and R. M. Shillito, Southwest Watershed Research Center, USDA-ARS, 2000 E. Allen Rd., Tucson, AZ 85719. (e-mail: goodrich@tucson.ars.ag.gov)

K. H. Syed, Department of Hydrology and Water Resources, University of Arizona, Tucson, AZ 85721.

D. A. Woolhiser, 1631 Barnwood Dr., Ft. Collins, CO 80525.

(Received December 17, 1996; revised April 9, 1997; accepted May 12, 1997.)